2018 European Control Conference (ECC)
June 12-15, 2018. Limassol, Cyprus

A Multi-Objective Nuclear Core Control Performing Hot and Cold Leg Temperature Control

L. Lemazurier, Ph. Chevrel, M. Yagoubi and A. Grossetête

***Abstract*— This paper proposes an innovative evolution of the current Pressurized Water Reactor (PWR) Nuclear Core Control strategies in order to satisfy more and more stringent maneuverability requirements. The following new control objectives are introduced: the hot and cold leg temperatures in contrast to the Average Coolant Temperature (ACT) in standard PWR control designs. This is made possible thanks to the use of the Primary Coolant Flowrate as a new control input. The proposed control design strategy first considers a point kinetic nuclear core non-linear model, calibrated on a highly realistic nuclear core simulation code. Secondly, it proceeds to a multi-objective H_2/H_∞ control synthesis, using an adequate control structure and non-smooth optimization.**

I. Introduction

In France, Nuclear Power Plants (NPP) are used during Flexible Operations, meaning that their load can be adapted to the electrical network demand. Flexibility has a substantial impact on Nuclear Core operations which are servo-controlled by the Core Control (CC) system. In most advanced Pressurized Water Reactor (PWR) designs, the CC objectives include the automatic control of the Average Coolant Temperature (ACT) and the Axial Offset (AO) (see [1], [2], [3] and references therein). In that case, the Control Rods are used as control inputs. As renewable energies are expected to rise importantly within the next decades, bringing a more fluctuating power demand in the electrical network, NPP flexibility may be impacted dramatically requiring enhanced performances for the CC. Therefore, the actual objectives might be reviewed to increase CC abilities according to emerging and more stringent requirements. In the context of this study, only Thermal Load Fatigue requirements are considered, namely the thermal fatigue (due to metal thermal expansion cycles) provoked by temperature variation cycles in the primary coolant during load transients. Renewable energies impact on the nuclear plant operations could be twofold: power fluctuations and amplitude increase in frequency control leading to greater instantaneous temperature variations as well as Load Cycling increase due to greater and more frequent transients [4]. Actual PWR core controls [1], [2] and [3] address temperature variations by controlling the ACT around a reference depending on a Part-Load diagram. Thus, Hot and Cold leg temperatures vary significantly with power during load transients. For instance, for an EPR (AREVA's latest PWR design) a load variation from 100% to 25% of Nominal Power induces a hot (resp. cold) leg temperature variation of 15 $°C$ (resp. 8 $°C$) whereas the ACT variation is only of 4 $°C$. Therefore, in order to have a greater control of the core temperatures and thus to reduce thermal fatigue, this study proposes to control separately the Hot and Cold Leg Temperatures, rather than ACT. Yet, in order to control both temperatures in the nuclear core, the Primary Coolant Flowrate needs to be considered as a new control input. Indeed, as the flowrate increases, at a fixed power, the difference between the hot and cold leg temperatures decreases (and conversely). Therefore, by means of the primary coolant flowrate in addition to Mode T control rods [2] (P_{bank} and H_{bank}) it is possible to control the hot and cold leg temperatures and the AO.

Actual PWR core controls are PID (Proportional-Integral-Derivative) based controllers which provide conform performances regarding standard core control [1], [2] and [3]. However, tuning PID based controllers is somehow hard, especially in the case of highly coupled Multiple-Inputs Multiple-Outputs (MIMO) systems. Thus, as new control features (hot and cold leg temperatures) are considered, this work investigates an advanced control strategy in order to gain maximum profit.

Multiple works have proposed innovative nuclear reactor control [5]. Using point kinetic core models [6] or one-dimensional two-node core models [7] and [8], core controllers have been designed based on various control techniques. Although some of these studies considered the AO control, none of them considered the hot and cold leg temperature control.

In a previous work [9], an innovative multi-objective H_2/H_∞ control design was proposed to control the ACT and the AO, using a Gain-Scheduled control strategy. Based on a point-kinetic non-linear nuclear core model, a set of LTI models were obtained around some fixed operating points depending on the nuclear core power level. It showed suitable performances over a wide power level operating range on the non-linear nuclear core model. It also proved that a LTI controller, designed at intermediate power (80% Nominal Power (NP)), provides suitable performances for a wide power range (from 60%NP to 90%NP). Yet, this previous work did not address Hot and Cold leg temperature control and did not benefit from a model endowed with Primary Flowrate variations ability.

Considering the preceding elements, the first contribution of this paper is to use an additional innovative actuator, the primary coolant flowrate, in order to control

L. Lemazurier PhD Student at Institut Mines Telecom (IMT) Atlantique, Nantes, France (Lori.Lemazurier@areva.com).
Ph. Chevrel, is with the Automatic Control Department at IMT Atlantique, Nantes, France (Philippe.Chevrel@imt-atlantique.fr).
M. Yagoubi, is with the Automatic Control Department at IMT Atlantique, Nantes, France (Philippe.Chevrel@imt-atlantique.fr).
A. Grossetête is with AREVA Reactor Process Department at AREVA NP, Paris La Défense, France (Alain.Grossetete@areva.com).

separately the Hot (T_h) and Cold (T_c) Legs temperatures of a PWR core. The authors would like to highlight the fact that, prior to this study, primary coolant flowrate was an untried solution for PWR core control. Indeed, it is normally considered constant for PWR reactors. It is used in addition to the control rods (P_{bank} and H_{bank}) displacement to enable AO control as well (please note that the Xenon effects, P_{max} control and Boron concentration adjustments (see [2]) will be discussed in a forthcoming work). The second contribution of the paper consists in an explicit characterization of the multi-objective control specifications (including robustness) using some specific H_2 and H_∞ transfer norms leading to a fixed structure controller with a parsimonious parameterization. The last contribution of the current paper is to simulate transients on the realistic MANTA/SMART [10] nuclear reactor simulation code, in order to test and validate the new control.

The remainder of this paper is organized as follows. Section II presents the linearized core model and discusses the different impacts of nuclear core operations on the varying parameters of the presented model. The multi-objective control strategy is described in Section III. Section IV shows and analyses the obtained simulation results. Finally, some concluding remarks take place in Section V.

Nomenclature

$(\delta)T_h$	*(*) Hot leg temperature in °C*
$(\delta)T_c$	*(*) Cold leg temperature in °C*
$(\delta)T_h^{SG}$	*(*) Hot Steam Generator input temperature in °C*
$(\delta)T_c^{SG}$	*(*) Cold Steam Generator output temperature in °C*
$(\delta)AO$	*(*) Axial Offset in %*
$(\delta)\rho_{dop}$	*(*) Reactivity induced by Doppler effect in pcm (**)*
$(\delta)n$	*(*) % of neutrons relative to nominal power (n_0)*
$(\delta)c$	*(*) % of precursors relative to nominal power (c_0)*
$(\delta)\rho$	*(*) reactivity in pcm*
$(\delta)P_{turb}$	*(*) Turbine power in W*
$(\delta)Q_p$	*Primary Coolant flowrate in m^3/s*
n_{eq}	*% of neutrons relative to nominal power at equilibrium*
P_{eq}	*Turbine power at equilibrium in W*
Q_{eq}	*Primary Coolant flowrate at equilibrium in m^3/s*
K_n	*Core power coefficient in W/% of neutrons*
C_p	*Primary coolant heat capacity in $W.s/°C/m$*
K_{ct}	*AO cold leg temperature coefficient in %AO/°C*
$K_{\delta t}$	*AO delta temperature coefficient in %AO/°C*
$K_{AO,P}$	*AO Pbank worth coefficient in %AO/steps*
$K_{AO,H}$	*AO Hbank worth coefficient in %AO/steps*
K_{dop}	*Doppler reactivity coefficient in pcm/neutrons*
K_h	*Hot leg temperature reactivity coefficient in pcm/°C*
K_c	*Cold leg temperature reactivity coefficient in pcm/°C*
$K_{\rho P}$	*Pbank reactivity worth insertion in pcm/step*
$K_{\rho H}$	*Hbank reactivity worth insertion in pcm/step*
τ_{core}	*Core response time in s*
τ_{cl}	*Cold leg response time in s*
τ_{AO}	*AO response time in s*
τ_{dop}	*Doppler response time in s*
τ_{hl}	*Hot leg response time in s*
τ_{SG}	*Steam Generator response time in s*
β	*Delayed neutrons fraction in pcm*
l^*	*Prompt neutrons lifetime in s*
λ	*Decay constant of precursors in s*
P_{bank}	*P_{bank} rod position in extracted steps*
H_{bank}	*H_{bank} rod position in extracted steps*
vP_{bank}	*P_{bank} rod speed in extracted steps /s*
vH_{bank}	*H_{bank} rod speed in extracted steps /s*

II. CORE MODEL

A. Linearized Model Description

In a previous work [9] a simplified non-linear nuclear core point kinetic model was proposed by the authors of the current paper. A linearized model has been deduced from the latter and is recalled here through equations (1) to (11) with a slight difference in equations (1) and (8) where the flowrate Q_p has been linearized through Taylor expansion.

Please note that δv represents the deviation of variable v about its equilibrium value v_{eq}. For instance, $n(t) = n_{eq} + \delta n(t)$ where δn is the deviation of n about the equilibrium value n_{eq}. Some of those model parameters (bold type coefficients in equations (1) to (11)) vary over time, i.e. with the nuclear reactor operations.

$$\frac{d\delta T_h}{dt}(t) = -\frac{1}{\tau_{core}}\delta T_h(t) + \frac{1}{\tau_{core}}\delta T_c(t) + \frac{1}{\tau_{core}}\frac{K_n}{\boldsymbol{Q_{eq}}C_p}\left(\delta n(t) - \frac{\boldsymbol{n_{eq}}}{\boldsymbol{Q_{eq}}}\delta Q_p(t)\right) \quad (1)$$

$$\frac{d\delta T_c}{dt}(t) = -\frac{1}{\tau_{cl}}\delta T_c(t) + \frac{1}{\tau_{cl}}\delta T_c^{SG}(t) \quad (2)$$

$$\frac{d\delta AO}{dt}(t) = -\frac{1}{\tau_{AO}}\delta AO(t) + \frac{1}{\tau_{cl}}\delta T_c^{SG}(t) + \frac{1}{\tau_{AO}}\left(\boldsymbol{K_{tc}}\delta T_c(t) + \boldsymbol{K_{dt}}\left(\delta T_h(t) - \delta T_c(t)\right)\right) + \frac{1}{\tau_{AO}}\left(\boldsymbol{K_{AO,P}}\delta P_{bank}(t) + \boldsymbol{K_{AO,H}}\delta H_{bank}(t)\right) \quad (3)$$

$$\frac{d\delta\rho_{dop}}{dt}(t) = -\frac{1}{\tau_{dop}}\delta\rho_{dop}(t) + \frac{\boldsymbol{K_{dop}}}{\tau_{dop}}\delta n(t) \quad (4)$$

$$\frac{d\delta n}{dt}(t) = -\frac{\beta}{l^*}\delta n(t) + \lambda\delta c(t) + \frac{\boldsymbol{n_{eq}}}{l^*}\rho(t) \quad (5)$$

$$\frac{d\delta c}{dt}(t) = \frac{\beta}{l^*}\delta n(t) - \lambda\delta c(t) \quad (6)$$

$$\frac{d\delta T_h^{SG}}{dt}(t) = -\frac{1}{\tau_{hl}}\delta T_h^{SG}(t) + \frac{1}{\tau_{hl}}\delta T_h(t) \quad (7)$$

$$\frac{d\delta T_c^{SG}}{dt}(t) = -\frac{1}{\tau_{SG}}\delta T_c^{SG}(t) + \frac{1}{\tau_{SG}}\delta T_h^{SG}(t) + \frac{1}{\tau_{sg}\boldsymbol{Q_{eq}}C_p}\left(\delta P_{turb}(t) - \frac{\boldsymbol{P_{eq}}}{\boldsymbol{Q_{eq}}}\delta Q_p(t)\right) \quad (8)$$

$$\frac{d\delta P_{bank}}{dt}(t) = vP_{bank}(t) \quad (9)$$

$$\frac{d\delta H_{bank}}{dt}(t) = vH_{bank}(t) \quad (10)$$

$$\rho(t) = \delta\rho_{dop}(t) + \boldsymbol{K_h}\delta T_h(t) + \boldsymbol{K_c}\delta T_c(t) + \boldsymbol{K_{\rho P}}\delta P_{bank}(t) + \boldsymbol{K_{\rho H}}\delta H_{bank}(t) \quad (11)$$

B. Varying parameters

This section aims at describing the different impacts of nuclear core operations on the varying (bold type) parameters in equations (1) to (11). Let us precise that the

core model will be considered on a limited power level operating range – from 60%NP to 90%NP – at a fixed fuel depletion (in our case the Beginning of Cycle). In these operating conditions, most of the varying parameters vary little or can be considered constant which will be discussed hereinafter.

The fixed fuel depletion and the limited power variations clearly induce low variations of the moderator (K_h and K_c) and Doppler (K_{dop}) effect parameters.

K_{tc}, K_{dt}, K_h and K_c depend on the Hot and Cold leg temperatures which need to be maintained at their references (control objectives), thus those parameters can be considered constant as well. Moreover, due to P_{bank} rod overlap (as in Mode T [1], [2] and [3] and low H_{bank} position variations in the considered limited operating range, the reactivity worth insertion parameters ($K_{\rho P}$ and $K_{\rho H}$) do not vary significantly under the limited operating hypothesis.

$K_{AO,P}$ and $K_{AO,H}$ are potentially sensitive to control rod positions in the core. Indeed, as an individual rod is inserted in the core, its effect on the AO varies significantly according to its position. In the upper part, a rod insertion decreases the AO whereas in the lower part, a rod insertion increases the AO. Nevertheless, between 60%NP and 90%NP P_{bank} benefits from rod overlap (several rods inserting simultaneously [1], [2] and [3]) which reduce dramatically the effect on the AO. Plus, in the considered conditions, H_{bank} position varies little which makes its effect on AO invariable. Therefore, $K_{AO,P}$ and $K_{AO,H}$ can also be considered constant.

Finally, P_{eq}, Q_{eq} and n_{eq} (respectively the turbine power, the flowrate and the neutron density at equilibrium) may vary during core operations. Due to limited operating range and the considered controlled objectives their variations are limited: 60% to 90% for P_{eq} and n_{eq} and 75% to 112% for Q_{eq}.

In conclusion, this section showed that most varying parameters can be considered constant considered operating conditions, although few parameters (P_{eq}, Q_{eq} and n_{eq}) may vary during the core transients. However, as their variations are limited and known, a LTI controller shall be able to control the nonlinear plant over the considered operating range, despite model errors, by means of sufficient robustness abilities.

C. State-Space representation

Let π be the vector gathering the previously discussed varying parameters as defined in equation (12).

$$\pi = (K_{tc} \quad K_{dt} \quad K_{AO,P} \quad K_{AO,H} \quad K_{dop} \quad K_h \quad K_c \quad K_{\rho P} \ldots \quad K_{\rho H} \quad n_{eq} \quad P_{eq} \quad Q_{eq})^T \tag{12}$$

According to the equations (1) to (11), it is possible to represent the simplified core model through a state space representation as in equation (13), resulting in a system G. Let x be the state, u_K the input, d the disturbance, z the output parameters and y the measured outputs of the system G. The matrices A, B_u, B_d, C_z, C_y, D_u^z, D_d^z, D_u^y and D_d^y are all of appropriate dimensions and detailed in appendix A.

Equation (15) shows two disturbances:

- d_1 the turbine power
- d_2 the input (control rods and Primary Flowrate) disturbances

$$(G)\begin{cases} \dot{x} = A(\pi)x + B_u(\pi)u_K + B_d(\pi)d \\ z = C_z(\pi)x + D_u^z(\pi)u_K + D_d^z(\pi)d \\ y = C_y(\pi)x + D_u^y(\pi)u_K + D_d^y(\pi)d \end{cases} \tag{13}$$

$$y = (y_1 \quad y_2)^T = (\delta T_h \quad \delta T_c \quad \delta AO \quad \delta n \quad \delta T_h \quad \delta T_c \quad \delta AO)^T \tag{14}$$

$$u_K = \begin{pmatrix} \delta Q_p \\ vP_{bank} \\ vH_{bank} \end{pmatrix} \qquad d = \begin{pmatrix} d_1 \\ d_2 \end{pmatrix} = \begin{pmatrix} \delta P_{turb} \\ d_{uQ} \\ d_{uP} \\ d_{uH} \end{pmatrix} \tag{15}$$

$$x = \begin{pmatrix} \delta T_h \\ \delta T_c \\ \delta AO \\ \delta \rho_d \\ \delta n \\ \delta c \\ \delta T_h^{SG} \\ \delta T_c^{SG} \\ \delta P_{bank} \\ \delta H_{bank} \end{pmatrix} \qquad z = \begin{pmatrix} z_1 \\ z_2 \\ z_3 \end{pmatrix} = \begin{pmatrix} \delta T_h \\ \delta T_c \\ \delta AO \\ d_Q + \delta Q_p \\ d_{uP} + vP_{bank} \\ d_{uH} + vH_{bank} \\ \delta Q_p vP_{bank} \\ vP_{bank} \\ vH_{bank} \end{pmatrix} \tag{16}$$

Equation (16) shows three outputs that will be used to design the controller:

- z_1 the controlled outputs: Hot Leg (T_h), Cold Led (T_c) and the Axial Offset (AO).
- z_2 the input (u_K) added to an input additive noise (d_2).
- z_3 the input (u_K).

III. Control Strategy

Let us now focus on the proposed control strategy. First, the structure of the controller is defined so that it is both simple and capable of reaching the control specifications. Secondly, a mathematical formalization of the control specifications (including robustness) in the form of criteria and constraints using H_2 and H_∞ norms is detailed. Finally, the multi-objective problem thus defined is solved using a well-suited non-smooth optimization solver.

A. Controller Structure

A controller with a parsimonious parameterization is chosen to facilitate both its readability and its synthesis. This is an output feedback of multiple gains and integrators. The integrators should guarantee zero static errors on the three controlled outputs, namely δT_h, δT_c and δAO. According to equation (13) the controller is defined as:

$$u_K = Ky = \begin{pmatrix} K_1 & K_2/s \end{pmatrix} \begin{pmatrix} y_1 \\ y_2 \end{pmatrix} \quad (17)$$

u_K being defined in equation (15), and $y_1 = (\delta T_h \ \ \delta T_c \ \ \delta AO \ \ \delta n)^T$ and $y_2 = (\delta T_h \ \ \delta T_c \ \ \delta AO)^T$ are being formed from y (see equation (14)). K_1 and K_2 are two gain matrices gathering all the decision variables of the underlying optimization problem. Let's remark that the structure is general enough to enable crossed integral actions on all actuators, from all outputs (i.e. components of y_2). The gain matrix K_2 is not necessarily diagonal. This would be too restrictive and may not allow an effective solution. It has to be of full rank however to guaranty zero-static errors on the controlled outputs (y_2) [11]. This generalizes the proposition of [12] and [13].

B. Control Problem Formulation

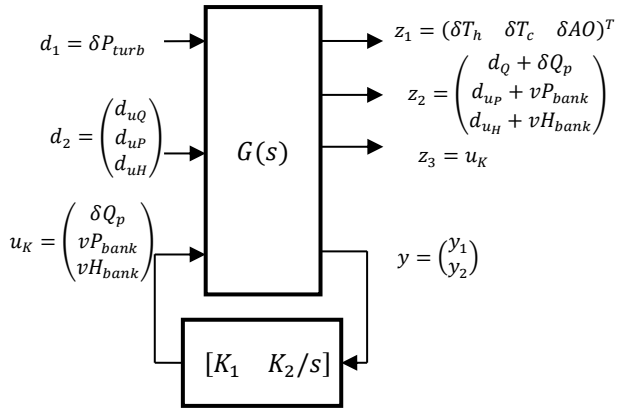

Figure 1: Standard Control scheme

$$\min_{K\in\Omega} \left\| W_1 T_{d_1 \to z_1} \right\|_2 \quad (18)$$

where Ω denotes the set of all stabilizing feedback gains of the form (17).

Let us first introduce the control problem from the standard control scheme as depicted in Figure 1. The control problem consists in determining K_1 and K_2 matrix coefficients in order to minimize a cost function and meets a set of constraints as defined hereinafter. The cost function is defined as the H_2 norm of the closed-loop transfer from disturbance (d_1) to the controlled signals (z_1) namely $T_{d_1 \to z_1}$. Minimizing this performance criterion (formalized in equation (18)) will make the turbine load variations have as less as possible impact on the controlled variables. W_1 (in eq. (18)) is a weighting filter, allowing to penalize much the low frequency deviation, thanks to weighed integrators:

$$W_1(s) = \begin{pmatrix} \frac{K_{T_h}}{s} & 0 & 0 \\ 0 & \frac{K_{T_c}}{s} & 0 \\ 0 & 0 & \frac{K_{AO}}{s} \end{pmatrix} \quad (19)$$

Constraints are now defined to ensure control robustness and actuator energy limitations. First, robustness is taken into account simply through the multivariable modulus margin (inverse of the infinity norm of the sensitivity function), denoted as M_m. The modulus margin is an efficient MIMO robustness indicator, because it measures resilience to simultaneous gain-phase uncertainties and also to bounded non-linearities (circle criterion [14]). The modulus margin constraint considered here is given by:

$$M_m = \frac{1}{\|S\|_\infty} = \frac{1}{\left\| T_{d_2 \to z_2} \right\|_\infty} \geq 0.5 = W_2 \quad (20)$$

where S denotes the sensitivity function. Note that the choice of the weighting gain W_2 means that we seek for a maximum peak of 6 dB on the sensitivity function. Therefore, the constraint can be written as:

$$\left\| W_2 T_{d_2 \to z_2} \right\|_\infty \leq 1 \quad (21)$$

In order to prevent unrealistic solicitations (actuator energy limitations) of the control rods (P_{bank} and H_{bank} speed saturation) and Primary Coolant Flowrate (e.g. flowrate amplitude variations), we chose to constraint the H_∞ norm of all three transfers between the disturbance d_1 and control inputs vP_{bank}, vH_{bank} and Q_p. The H_∞ norms considered are weighted through gains W_3, and W_4 as indicated in equations (21), (22) and (23). The maximum possible gain between the input and the output considered is thus imposed.

$$\left\| W_3 T_{d_1 \to vP_{bank}} \right\|_\infty \leq 1 \quad (22)$$

$$\left\| W_3 T_{d_1 \to vH_{bank}} \right\|_\infty \leq 1 \quad (23)$$

$$\left\| W_4 T_{d_1 \to Q_p} \right\|_\infty \leq 1 \quad (24)$$

Finally, the optimization problem can be summarized as follows:

$$\begin{cases} \min_{K\in\Omega} \left\| W_1 T_{d_1 \to z_1} \right\|_2 \\ \left\| W_2 T_{d_2 \to z_2} \right\|_\infty \leq 1 \\ \left\| W_3 T_{d_1 \to vP_{bank}} \right\|_\infty \leq 1 \\ \left\| W_3 T_{d_1 \to vH_{bank}} \right\|_\infty \leq 1 \\ \left\| W_4 T_{d_1 \to Q_p} \right\|_\infty \leq 1 \end{cases} \quad (25)$$

C. Optimization algorithm

The optimization problem presented in the previous section involves a MIMO H_2/H_∞ multi-objective structured controller. The underlying optimization problem is non-convex and non-smooth. Rather than trying to approach it through convex relaxation and LMI solvers, our choice is to solve it directly via dedicated non-smooth optimization. Such an approach gains in popularity because it does not involve conservatism when achieving the global optimum. In control, these approaches were initiated by Pierre Apkarian and Dominikus Noll in [15], [16] and [17]. It is now available through *Systune* solver (Matlab R2014a). In the sequel, the presented results were obtained thanks to this solver.

IV. Simulation

A. Operating Conditions

The simulations that will be performed in the following sections will consider a Beginning of Cycle nuclear core at intermediate power levels: between 60% and 90% of the

nominal Nuclear Core power. In fact, at higher power levels: between 90% and 100% of nominal power, as the control rods are in the upper core part, the core control requires the action of the Boron concentration variations in order to guarantee correct performances [1], [2] and [3]. This power level range will be discussed in a forthcoming work.

B. Core Control Requirements

The core controller that will be designed in the following section is expected to meet the following requirements:

- T_h deviation shall not exceed 1.5 ° C: $|\delta T_h| < 1.5°C$
- T_c deviation shall not exceed 1.5 ° C: $|\delta T_c| < 1.5°C$
- AO deviation shall not exceed 5%: $|\delta AO| < 5\%$
- The Core Control shall be able to perform 5% Nominal Power ramp and 10% Nominal Power step variations with respect to the previous requirements
- The maximum P_{bank} and H_{bank} rod speeds is 75 steps per minute

C. Simulation scenario assumptions

The two following scenarii will be simulated:

- Scenario 1: 5%NP/min ramp load variation
- Scenario 2: 10%NP step load variation using this model

These simulations are carried out on the closed loop system, composed of the highly realistic nuclear reactor simulation code (MANTA/SMART [10]) and a single LTI controller designed according to a linearized plant model. The model was extracted from the system described in part II for a fixed vector π defined at 80% NP.

TABLE I describes the core operating conditions at 80% NP considered at equilibrium for the simulation (e.g.at 80% NP, the Hot Leg temperature T_h is at 326 °C). Thus, the designed H_2/H_∞ multi-objective controller aims at maintaining the controlled parameters about those values which is equivalent to controlling their deviations (δT_h , δT_c and δAO) about zero.

TABLE I. CORE CONFIGURATION

Core Configuration at 80% NP			
Control Objectives	T_h	T_c	AO
Values	326 °C	299 °C	3 %
Actuators	P_{bank}	H_{bank}	Q
Values	790 extracted steps	391 extracted steps	100 %

D. Simulation scenario 1: 5%NP/min ramp

Figure 2, Figure 3 and Figure 4 present the scenario 1 simulation results. Basically, the turbine power varies from 80%NP to 60%NP at a speed of 5%NP per minute. Figure 2 shows that the controlled parameters (T_c, T_f and AO) deviations suitably converge to zero (thus static errors are rejected) and do not exceed the required maximum 1.5°C for the temperatures and 5% for the AO amplitudes. Figure 3 shows the control rods position deviations (δP_{bank} and δH_{bank}) about their equilibrium ($P_{bank} = 790$ steps and $H_{bank} = 391$ steps). It also shows the Flowrate (Q_p) variation during the transient period. Figure 4 shows that the control rod speeds do not exceed the maximum authorized rod speed of 75 steps/min since the maximum rod speed is about 24 steps/min.

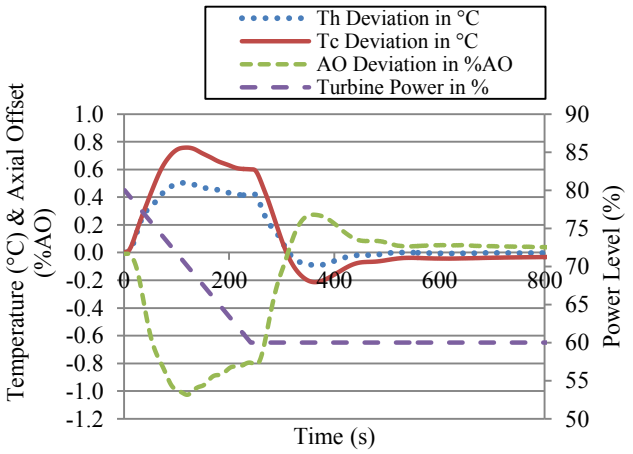

Figure 2: T_c, T_h and AO deviations - 5%NP/min ramp

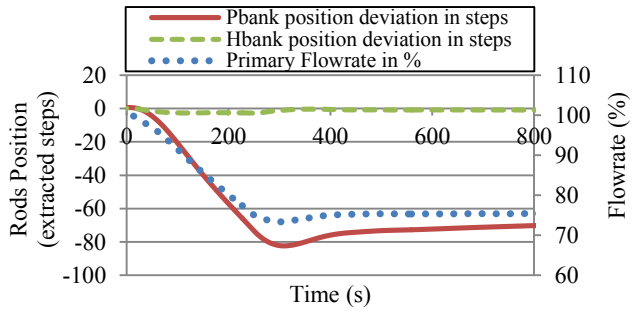

Figure 3: Rods and Flowrate variations - 5% NP /min ramp

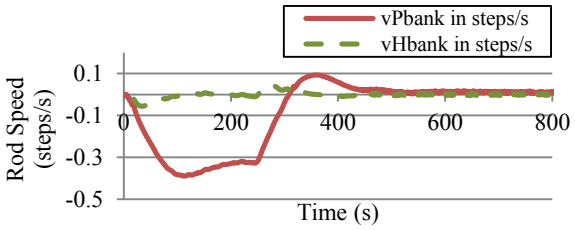

Figure 4: Control Rods speeds - 5%NP/min ramp

In order to evaluate the hereinabove results, the same transient was performed with the multi-objective H_2/H_∞ controller designed in [9]. This controller aims at controlling ACT and AO by means of P_{bank} and H_{bank} actuators (without Flowrate variations) and already provides optimized performances compared to existing controllers for comparable objectives. Please note the work in [9] only showed results on a simplified non-linear Core model

whereas the present study provides results on MANTA/SMART [10] simulation code which is far more realistic.

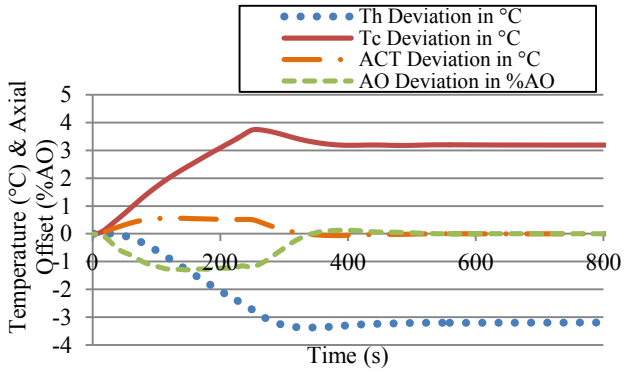

Figure 5: T_c, T_h, *ACT* and *AO* deviations - 5%NP/min ramp – without T_c and T_h control

The results are presented in Figure 5. It shows that ACT and AO are controlled. T_h and T_c temperatures deviate by about 3°C from their references, respectively 325°C and 298°C, basically due to a power variation (80%NP to 60%NP) at constant flowrate.

Compared to the controller in [9] (Figure 5), the proposed control in the present paper (Figure 2) shows an improvement in the way that both T_h and T_c are controlled separately about their references. Therefore a load variation has low impact on either Hot or Cold leg temperatures. Plus, the AO is controlled as well as for other control schemes.

E. Simulation scenario 2: 10%NP step

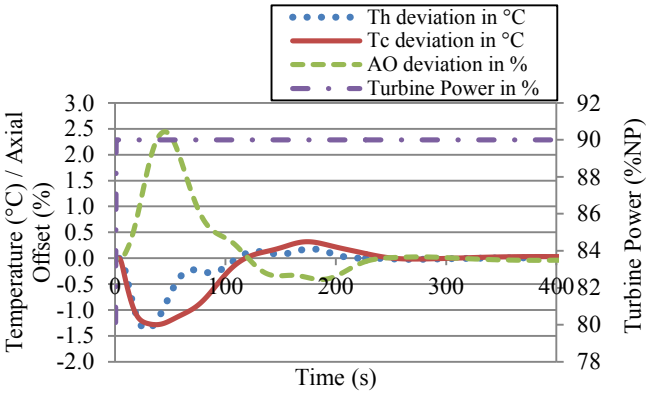

Figure 6: T_c, T_h and *AO* deviations – 10% NP step

Figure 6 presents the scenario 2 simulation results. The H_2/H_∞ multi-objective controller shows, once more, good performances (in comparison to chosen objectives and constraints) since neither Hot and Cold leg temperatures nor Axial Offset overpass their maximum deviation limits and they have no static errors. Please note that the control rod speeds have been checked and do not exceed 43.8 steps/min, which is congruent with the maximum possible control rod speed (75 steps/min).

As in the previous section, in order to evaluate results, the same transient was applied with the controller that controls ACT and AO only (as in [9]). Results are presented in Figure 7. It shows that the T_h and T_c temperatures transiently deviate by up to 3°C from their references whereas in the case of the designed controller (Figure 6), both T_h and T_c temperatures deviate by less than 1.5°C from their references. Thus, as it was concluded in the previous section, the designed controller provides significant improvement since the core temperatures are less impacted by power variations.

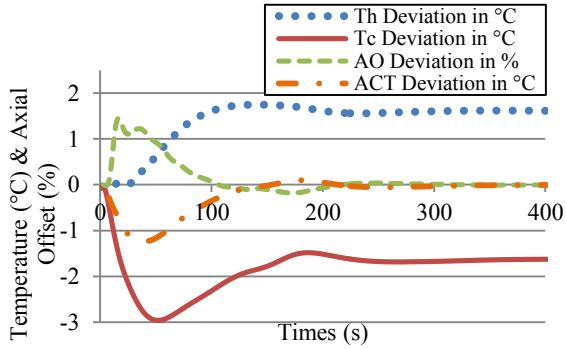

Figure 7: T_c, T_h, *ACT* and *AO* deviations - 5%NP/min ramp – without T_c and T_h control

According to both of the presented simulation results, the synthesized LTI controller provides correct robustness performances as it controls the system along a large operating range (between 60% NP and 90% NP) even if the plant has a non-linear behavior.

V. Conclusion

This study aimed at synthesizing a H_2/H_∞ multi-objective Nuclear Core controller based on a LTI model corresponding to the system behavior at 80% of the nominal power. The considered model was identified over a highly realistic core simulation code (MANTA/SMART [10]). An innovating problem was then addressed as it considered the Primary Coolant Flowrate as a new control input (acting in addition to standard core control actuators), allowing to meet new control objectives. These objectives were to control separately Hot and Cold Leg Temperatures (instead of average coolant temperature in most standards PWR) besides Axial Offset. This innovative control would enable in particular to minimize temperature variations and thus reduce Thermal Load Fatigue.

The controller showed great performances. When simulated on MANTA/SMART [10], characterized control specifications were all correctly fulfilled: no static errors, conform controlled parameters deviations and correct actuator solicitations. The controller revealed good robustness as it controlled correctly the plant over the considered operating range (60%NP to 90%NP) even if it is non-linear. The results were confronted to standard core control strategies and proved a significant improvement as the hot and cold leg temperature deviations were significantly lower with the new controller.

In a forthcoming work we propose to apply the same method, as presented in this study, to various operating

points to design a gain-scheduled controller, as in [9], to cover the complete operating range, and furthermore, introduce the Xenon dynamics, P_{max} control and Boron concentration actuation.

APPENDIX

$$A = \begin{pmatrix} -\frac{1}{\tau_{core}} & \frac{1}{\tau_{core}} & 0 & 0 & \frac{K_n}{C_p Q_n \tau_{core}} & 0 & 0 & 0 & 0 & 0 \\ 0 & -\frac{1}{\tau_{cl}} & 0 & 0 & 0 & 0 & 0 & \frac{1}{\tau_{cl}} & 0 & 0 \\ \frac{K_{dt}}{\tau_{AO}} & \frac{K_{ct}-K_{dt}}{\tau_{AO}} & -\frac{1}{\tau_{AO}} & 0 & 0 & 0 & 0 & 0 & \frac{K_{AO,P}}{\tau_{AO}} & \frac{K_{AO,H}}{\tau_{AO}} \\ 0 & 0 & 0 & -\frac{1}{\tau_{dop}} & \frac{K_{dop}}{\tau_{dop} n_{eq}} & 0 & 0 & 0 & 0 & 0 \\ \frac{K_h n_{eq}}{l^*} & \frac{K_c n_{eq}}{l^*} & 0 & \frac{n_{eq}}{l^*} & -\frac{\beta}{l^*} & \lambda & 0 & 0 & K_{\rho P}\frac{n_{eq}}{l^*} & K_{\rho H}\frac{n_{eq}}{l^*} \\ 0 & 0 & 0 & 0 & \frac{\beta}{l^*} & -\lambda & 0 & 0 & 0 & 0 \\ \frac{1}{\tau_{hl}} & 0 & 0 & 0 & 0 & 0 & -\frac{1}{\tau_{hl}} & 0 & 0 & 0 \\ 0 & 0 & 0 & 0 & 0 & 0 & \frac{1}{\tau_{SG}} & -\frac{1}{\tau_{SG}} & 0 & 0 \\ 0 & 0 & 0 & 0 & 0 & 0 & 0 & 0 & 0 & 0 \\ 0 & 0 & 0 & 0 & 0 & 0 & 0 & 0 & 0 & 0 \end{pmatrix}$$

$$B_u = \begin{pmatrix} -\frac{K_n n_{eq}}{\tau_{core} Q_{eq} C_p} & 0 & 0 \\ 0 & 0 & 0 \\ 0 & 0 & 0 \\ 0 & 0 & 0 \\ 0 & 0 & 0 \\ 0 & 0 & 0 \\ -\frac{P_{eq}}{\tau_{SG} Q_{eq} C_p} & 0 & 0 \\ 0 & 1 & 0 \\ 0 & 0 & 1 \end{pmatrix} \quad B_d = \begin{pmatrix} 0 & -\frac{K_n n_{eq}}{\tau_{core} Q_{eq} C_p} & 0 & 0 \\ 0 & 0 & 0 & 0 \\ 0 & 0 & 0 & 0 \\ 0 & 0 & 0 & 0 \\ 0 & 0 & 0 & 0 \\ 0 & 0 & 0 & 0 \\ \frac{1}{\tau_{SG} Q_{eq} C_p} & -\frac{P_{eq}}{\tau_{SG} Q_{eq} C_p} & 0 & 0 \\ 0 & 0 & 1 & 0 \\ 0 & 0 & 0 & 1 \end{pmatrix}$$

$$C_z = \begin{pmatrix} 1 & 0 & 0 & 0 & 0 & 0 & 0 & 0 & 0 & 0 \\ 0 & 1 & 0 & 0 & 0 & 0 & 0 & 0 & 0 & 0 \\ 0 & 0 & 1 & 0 & 0 & 0 & 0 & 0 & 0 & 0 \\ 0 & 0 & 0 & 0 & 0 & 0 & 0 & 0 & 0 & 0 \\ 0 & 0 & 0 & 0 & 0 & 0 & 0 & 0 & 0 & 0 \\ 0 & 0 & 0 & 0 & 0 & 0 & 0 & 0 & 0 & 0 \\ 0 & 0 & 0 & 0 & 0 & 0 & 0 & 0 & 0 & 0 \\ 0 & 0 & 0 & 0 & 0 & 0 & 0 & 0 & 0 & 0 \\ 0 & 0 & 0 & 0 & 0 & 0 & 0 & 0 & 0 & 0 \end{pmatrix}$$

$$C_y = \begin{pmatrix} 1 & 0 & 0 & 0 & 0 & 0 & 0 & 0 & 0 & 0 \\ 0 & 1 & 0 & 0 & 0 & 0 & 0 & 0 & 0 & 0 \\ 0 & 0 & 1 & 0 & 0 & 0 & 0 & 0 & 0 & 0 \\ 0 & 0 & 0 & 0 & 1 & 0 & 0 & 0 & 0 & 0 \\ 1 & 0 & 0 & 0 & 0 & 0 & 0 & 0 & 0 & 0 \\ 0 & 1 & 0 & 0 & 0 & 0 & 0 & 0 & 0 & 0 \\ 0 & 0 & 1 & 0 & 0 & 0 & 0 & 0 & 0 & 0 \end{pmatrix}$$

$$D_u^z = \begin{pmatrix} 0 & 0 & 0 \\ 0 & 0 & 0 \\ 0 & 0 & 0 \\ 1 & 0 & 0 \\ 0 & 1 & 0 \\ 0 & 0 & 1 \\ 1 & 0 & 0 \\ 0 & 1 & 0 \\ 0 & 0 & 1 \end{pmatrix} \quad D_d^z = \begin{pmatrix} 0 & 0 & 0 & 0 \\ 0 & 0 & 0 & 0 \\ 0 & 0 & 0 & 0 \\ 0 & 1 & 0 & 0 \\ 0 & 0 & 1 & 0 \\ 0 & 0 & 0 & 1 \\ 0 & 0 & 0 & 0 \\ 0 & 0 & 0 & 0 \\ 0 & 0 & 0 & 0 \end{pmatrix}$$

$$D_u^y = \begin{pmatrix} 0 & 0 & 0 \\ 0 & 0 & 0 \\ 0 & 0 & 0 \\ 0 & 0 & 0 \\ 0 & 0 & 0 \\ 0 & 0 & 0 \\ 0 & 0 & 0 \\ 0 & 0 & 0 \end{pmatrix} \quad D_d^y = \begin{pmatrix} 0 & 0 & 0 & 0 \\ 0 & 0 & 0 & 0 \\ 0 & 0 & 0 & 0 \\ 0 & 0 & 0 & 0 \\ 0 & 0 & 0 & 0 \\ 0 & 0 & 0 & 0 \\ 0 & 0 & 0 & 0 \\ 0 & 0 & 0 & 0 \end{pmatrix}$$

REFERENCES

[1] A. Grossetête, "Le pilotage de l'EPR : mode T". *Revue Générale du Nucléaire*, 2007, pp. 37-41.

[2] A. Grossetête, « EPR: high load variation performances with the "Tmode" core control". *International Congress on Advances in Nuclear Power Plants*, vol. 42, 2008, pp. 21-25.

[3] A. Grossetête, "ATMEA1&EPR mode T Core Control Innovative Features for High Operating Flexibility". *Transactions of the American Nuclear Society*, 2014, pp. 1095-1098.

[4] N. Troy, "Base-Load Cycling on a System With Significant Wind Penetration". *IEEE Transactions on Power Systems*, vol. 25, 2010, pp. 1088-1097.

[5] G. Li, "Modeling and control of nuclear reactor cores for electricity generation: A review of advanced technologies". *Renewable and Suitable Energy Reviews*, vol. 60, 2016, pp. 116-128.

[6] H. Arab-Alibeik, "Improved Temperature Control of a PWR Nuclear Reactor Using an LTQ/LTR Based Controller". *IEEE Transactions on Nuclear Science*, vol. 50, 2003, pp. 211-218.

[7] D. C. Bauer and C. Poncelet, "Practical Xenon Spatial Control". *Nuclear Technology*, vol. 21, 1974, pp. 165-189.

[8] Y. Zhang, "Improvement of core control strategy for CPR1000: Load follow without boron adjustment". *Progress in Nuclear Energy*, vol. 81, 2015, pp. 98-103.

[9] L. Lemazurier, M. Yagoubi, Ph. Chevrel and A. Grossetête, "Multi-Objective H_2/H_∞ Gain-Scheduled Nuclear Core Control Design *IFAC World Congress*, Toulouse, 2017.

[10] M. Gonnet, A. Haulbert and M. Canac, "Nuclear Plant Simulation Using Three-Dimensional Core Modeling". *IAEA INIS Collection*, http://www.iaea.org/inis/collection/NCLCollectionStore/_Public/35/106/35106377.pdf.

[11] W.M. Wonham, "Linear Multivariable Control: a Geometric Approach". *Springer*, 1985.

[12] D. Garcia, A. Karimi and R. Longchamp, "Robust PID Controller Tuning with Specification on Modulus Margin". *American Control Conference*, 2004, pp. 3297-3302.

[13] K. J. Astrom, H. Panagopoulos and T. Hagglund, "Design of PI Controllers based on Non-Convex Optimization". *Automatica*, vol. 34, 1998, pp. 585-601.

[14] M. G. Safonov, "A Multiloop Generalization of the Cirlce Criterion for Stability Margin Analysis". *IEEE Transactions on Automatic Control*, vol. AC-26, 1981, pp. 415-422.

[15] P. Apkarian, and D. Noll, "Nonsmooth H_∞ Synthesis". *IEEE Transactions on Automatic Control*, vol. 51, 2006, pp 71–86.

[16] P. Apkarian, and D. Noll, "Nonsmooth optimization for multidisk H_∞ synthesis". *European Journal of Control*, vol. 12, 2006, pp. 229–244.

[17] P. Apkarian, D. Noll and P. Rondepierre, "Mixed H_2/H_∞ Control via Nonsmooth Optimization". *SIAM J. Control and Optimization*, vol. 47, 2008, pp. 1516–1546.